AIAA JOURNAL
Vol. 47, No. 4, April 2009

Approach for Increasing the Static Dimensional Stability of Composite Space Structures

Mark R. Garnich,* P. Liu,† and V. M. K. Akula
University of Wyoming, Laramie, Wyoming 82071
John F. Fitch‡
ATK Space Systems, Inc., San Diego, California 92121
and
David S. Long§
ATK Space Systems, Inc., Magna, Utah 84044

DOI: 10.2514/1.40349

Dimensional stability is an important performance parameter for many space structures. The concept of "antidistortion appliqués" was developed for minimizing thermally induced dimensional instability. The concept involves adding material to offset and eliminate measured instabilities. A computational framework was developed that uses experimental data characterizing the adverse thermal distortions. The computations include a finite element model that embodies the idealized thermoelastic properties of the structure in conjunction with optimization software that drives iterations of the characteristics of the antidistortion appliqués within the finite element model. In a modeling only study, it was predicted that distortions could be reduced in some cases by more than 90%. In the combined experimental/computational study, the models predicted a 62% reduction in the objective function that characterized the adverse distortions, whereas the experiment that used the appliqué design generated by the analysis recorded a 78% reduction. The difference can be attributed to several factors. Adjustment of material properties due to manufacturing variations are routinely needed to correlate analytical predictions to match experiment results. Inherently thermal elastic distortion measurements require some level of data adjustment due to the problem of maintaining a reference, which, in itself, does not change shape due to thermal changes.

I. Introduction

THE technical challenge of precision space structures is to establish and maintain the geometric precision of equipment that relies on precise geometry for operational performance. Dimensional instabilities can be static or dynamic. The primary focus of this work was the static instability associated with thermal strains.

Thermal instabilities occur as a result of either gradients in material properties in concert with a uniform temperature change, gradients in temperature in concert with nonzero thermal expansion properties, or combinations of both. Therefore, a structure with a uniform zero coefficient of thermal expansion (CTE) would eliminate both sources of thermal instability. Because this is not possible, the ultimate minimization of thermal instabilities would come from a combination of materials and design methodology that would enable the extremely fine control of the thermal deformation behavior in mass efficient composite structures.

Perhaps the single greatest advance in the technology of dimensionally stable space structures was the design of graphite fiber composite laminates that achieve a nominally zero in-plane CTE. With the use of sufficiently high modulus graphite fibers and proper laminate design, the "zero" CTE can be unidirectional or isotropic in the plane of the laminate. The CTE of the fiber, matrix, and individual lamina effectively interact so that a theoretical CTE of zero is possible. In practice, CTE less than 1 ppm/°C are routine and can be controlled to less than 0.1 ppm/°C in a single dimension. The transverse, or through thickness, CTE remains large (~20 ppm/°C) and is problematic in complex structures where its effects are generally unavoidable. This basic technology was developed and applied to a number of space structures in the 1970s (e.g., Prunty [1]). Since then, only incremental improvements have been made in space structure thermal stability.

In some cases where difficult stability criteria are to be met, a brute force approach is employed. That is, multiples of each of the structure components or subassemblies are fabricated so that, through individual testing, the best of the batch (e.g., lowest CTE) can be selected for use in the structure. For example, Maji et al. [2], who designed a spider truss support structure for a system of mirrors in an optical telescope, found that their pultruded graphite-epoxy truss members had a CTE that ranged from about 0.1 to 0.3 ppm/°C. They attributed the scatter to statistical variations in fiber misalignment and fiber volume fraction. Though effective, this method of testing and selecting only the best parts is clearly wasteful and does nothing to address the problems associated with subsequent joining.

Dodson and Rule [3] discussed some important factors affecting thermal stability of space flight optical benches. Their analysis of graphite/epoxy benches has indicated the selection of core types in sandwich structures, typical joint configurations, adhesive effects, and moisture effects are all important considerations in design. Shin et al. [4] have analyzed the thermal distortion of an orbiting solar array including composite material degradation effects. It was observed in their study that the strength, stiffness, and CTE of graphite/epoxy composite materials after exposure to simulated low-Earth-orbit environments decreased in proportion to increasing thermal cycles. It was also found that the solar arrays with composite face sheets were advantageous in view of weight savings, temperature distribution, and thermal distortion when compared to those with aluminum face sheets. In a discussion on the design of composite surrogate mirror support structure, Maji et al. [2] analyzed the mirror surface figure errors caused by temperature fluctuation and suggested a design to be a good one if it achieves the best balance between mass, dynamic properties, and thermal deformation.

Received 13 August 2008; revision received 19 December 2008; accepted for publication 24 December 2008.

*Department 3295, 1000 East University Avenue; Garnich@uwyo.edu. Member AIAA (Corresponding Author).

†Department 3295, 1000 East University Avenue; currently Global Engineering and Materials, Inc., 9 Goldfinch Terrace, East Lyme, Connecticut 06333.

‡9617 Distribution Avenue.

§7812 West 4100 South, Mail Stop UT03-HTS1.

To minimize the thermal deformation, it is generally accepted that materials with minimum CTE should be used. As early as the late 1970s, Prunty [1] discussed several types of dimensionally stable graphite composites for spacecraft structures. He suggested that the adoption of composites for planned spacecraft structures can achieve significant benefits in stiffness-critical and strength-critical applications and can be a virtual necessity where extreme dimensional stability is required. Carbon-fiber-reinforced polymers (CFRP) with high specific strengths, moduli, and design flexibility are highly developed and used frequently as structural materials of modern aircraft and spacecraft. Through proper design, it is not only possible to have near-zero CTE, but also to design the CTE of the composite to match that of other system components to minimize thermal mismatch and the resulting thermal distortions.

Grimaldi et al. [5] have discussed several types of composite materials in designing satellite antenna structures. All the composite materials used for antenna structures share the need for high strength and low CTE. Ishikawa et al. [6] have analyzed the thermal behavior of graphite-epoxy laminates with almost null coefficients of thermal expansion under a wide range of temperature. They proposed a lamination tailoring technique to control the CTE of graphite-epoxy composites. This technique consists of two concepts of the thermoelastic invariants and the lamination parameters. More recently, Bansemir and Haider [7] have reviewed the development of fiber composite structures for space applications. They argue that improvement of materials evaluation methods and analysis techniques can be applied for optimal tradeoffs between properties such as CTE, elastic modulus, and thermal conductivity in fiber-reinforced composites.

Previous research in design of structures to achieve higher levels of dimensional stability has taken a completely different approach than was taken in this project. Most previous work has been performed from a local perspective, where initial design and fabrication flaws were identified and attempts are made to minimize them. That is, the locations of problematic deformation, or issues of laminate design, are isolated and the designer attempts to devise a strategy to reduce or eliminate that local source (e.g., Dodson and Rule [3], Yoon and Kim [8], Bansemir and Haider [7], and Farmer et al. [9]). For example, the anisotropic CTE causes an angle change in curved laminates during a temperature change (Yoon and Kim [8]).

The approach discussed here was to design from a global perspective while employing cost-effective local strategies associated with current practice. The global approach reduces the thermal instabilities after initial fabrication and assembly. This was demonstrated through a combination of experiments and modeling. The experiments characterized the nature of overall thermal deformations due to uniform temperature change and the models devise a set of antidistortion appliqués that create offsetting thermal deformations. In effect, this creates offsetting forces within the structure in much the same way that the constituent materials and lamina do at the local material scales when designed for a net CTE of zero. A clear advantage of this approach is that adjustments can be made after initial fabrication so that success in meeting CTE requirements is not reliant on the level of initial perfection in materials and construction. The significant disadvantage is that it requires experimental deformation measurement technology that matches the performance objectives. As the precision requirement of structures increase, so do the costs of the methods required to verify their performance.

II. Anti-Distortion Appliqué Approach

A. Methodology

Intentional introduction of material may be used to work in a beneficiary way. That is, structures can improve their static or dynamic performance through purposely designed and strategically located material additions which can cancel effects from unwanted manufacturing imperfections. Here, these material additions are to cancel unwanted thermal deformations and are referred to as antidistortion appliqués. This paper presents a study of how the static dimensional stability of structures can be improved by the use of antidistortion appliqués.

A joint structure which can be found within composite space structures was taken as a demonstration problem. The basic approach consisted of a three-phase analysis. First, a finite element model to embody the joint idealized thermomechanical character of the structure was developed using the finite element analysis (FEA) software ABAQUS. In all cases, the deflections were small and geometrically linear analysis was conducted. Second, the actual part was tested in the laboratory under a simulated operating environment to measure the adverse thermal distortions. In this case, that meant raising and then lowering the temperature to simulate a large temperature change as can occur in the cryogenic environment of space. Finally, the finite element model was exercised repeatedly as needed with material additions (antidistortion appliqués) with the objective of eliminating the unwanted distortions. In simple cases, this last step might be conducted by trial and error by an analyst. However, for more general application, an optimization study can be automated with software that is adapted to modify and rerun the FEA repeatedly until an optimized configuration of antidistortion appliqués has been achieved. This last step was accomplished using the VisualDoc [10] software which interrogates a text output file from the FEA and then modifies a text input file for the next FEA based on an optimization algorithm that seeks to minimize an objective function based on the output. In this case, the objective function involves displacements that quantify the distortion.

B. Joint Structure

This research used a composite T-joint with reinforcing clips as a model problem to demonstrate the concept of antidistortion appliqués. Figure 1 shows the basic configuration of the composite T-joint structure. The horizontal and vertical composite plates consist of CFRP laminates. The two curved clips are also CFRP laminates used to connect the flat plates. Thin film adhesives that connect the plates with the clips were explicitly included in the models. The structure is assumed to sustain a uniform temperature change. The ABAQUS software provides different mathematical options for modeling such 3-D thin structures. Either shell element or continuum element formulations can be selected to perform the analysis. Depending on the thickness of modeled components, the two types of elements can be used alternatively, but generally, for laminated composite structures, the shell elements are numerically

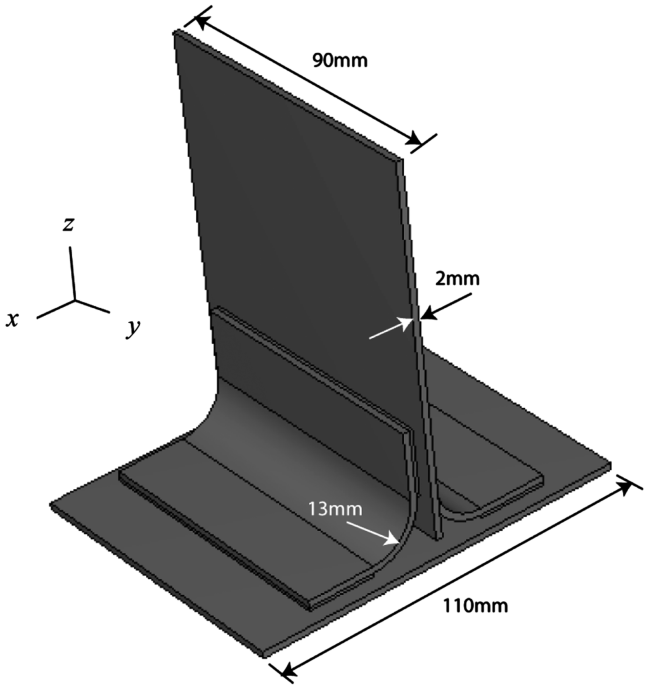

Fig. 1 Basic T-joint structure with nominal dimensions.

much more efficient. Because only displacements were of interest, there was no concern for the accuracy of local strains and stresses predicted by these models.

In this research, a couple of different laminates were assumed for different modeling exercises. Through a certain combination of fiber volume fraction and ply angles it is possible to achieve a theoretical null CTE for the in-plane material behavior (Ishikawa et al. [6]). The specific properties used are defined for each of the models discussed next. A material with 62% fiber volume fraction and ply thickness of 0.127 mm was first applied. The mechanical and thermal parameters of the composite (Matthews et al. [11]) were as follows: $E_{11} = 132$ GPa, $E_{22} = 10.8$ GPa, $v_{12} = 0.30$, $v_{23} = 0.59$, $G_{12} = 5.61$ GPa, $G_{23} = 3.17$ GPa, $\alpha_{11} = -0.77$ ppm, and $\alpha_{22} = 25$ ppm. The adhesives were assumed to be isotropic with a Young's modulus of 6.0 GPa and a Poisson's ratio of 0.3. The CTE α of the adhesive was taken as 54 ppm/°C.

C. Simulated Thermal Distortions

One of the attractive features of the antidistortion appliqué methodology is that you do not need to know the source of the distortions, only that they are manifest by the application environment which must be known. However, the method does require actual distortion data. In the absence of experimental data, simulated data can be used to demonstrate the method. Hence, the FEA was used to predict distortions due to an assumed defect in manufacture. It is emphasized that in practice the models would be idealizations of the structure with no attempt to capture defects due to manufacturing imperfections. Here, however, we have simulated a defect to demonstrate the methodology. Specifically, it was assumed that the two clips on the opposite sides of the vertical plate were misaligned. Figure 2 illustrates the exaggerated distortion of the vertical plate due to clip dislocation. Note that, in all deformed meshes, the displacements have been scaled to magnify them and make the distortions visible in the figures.

What deformations are adverse to a structure's performance will be application dependent. In this case, the difference between the x-axis displacements of the two top corner nodes was to be minimized. To highlight the effect of clip misalignment on the thermal distortion, a laminae structure with 8-ply orientation $[0/30/-30/90]_s$ was studied where the 0 deg fibers lie in the x-z plane of the coordinate system shown in Fig. 1. If no manufacturing defects exist, this arrangement of the orientation generates only symmetric thermal deformation and no distortion. With the effect from the misalignment, the joint's thermal distortion is directly related to how much the two clips are misaligned. For example, a clip misalignment of 2 mm resulted in a distortion parameter of 0.02572; for 6 mm it was 0.05376, and for 10 mm it was 0.07152.

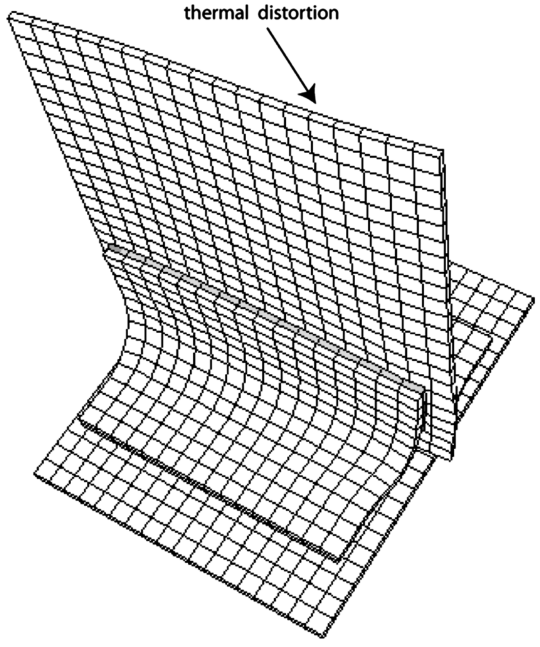

Fig. 2 Distortion (deformed FE mesh) due to the clip dislocation and thermal loading.

D. Antidistortion Appliqués by Trial and Error

With the present joint structure being relatively simple in geometry and the sources of the distortions known, using a trial-and-error approach is possible to test some appliqués. For the case in which there exists dislocation between the two clips, it was found that if two strips were attached to the plate with a dislocation also existing between them, then they will generate the required offsetting effect, which just cancels that caused by the clip dislocation. This result is illustrated in Fig. 3.

The trial-and-error approach works easily only for simple structures where the deformation is not too complicated and especially when the source of the deformation is known. But even for such simple structures, trial and error can be an inefficient approach. Considering the numerous possibilities of various appliqué shapes and locations, a trial-and-error approach may not yield the best design of appliqués quantitatively or it may be very time consuming. For more complicated structures, parametric optimization analysis is preferred. In the following section, an optimization study is discussed, still using the joint structure as an example.

E. Use of Optimization Software

Here, the design optimization was performed with ABAQUS working jointly with the optimization software VisualDOC [10]. ABAQUS is used for the thermomechanical analysis, and VisualDOC provides numerical tools to search for the best array of appliqué parameters. Among the different algorithms used to find the optimum solution of an objective function, the methods in VisualDOC can be classified as gradient-based and non-gradient-based approaches. Gradient-based approaches employ the standard strategy of first calculating the derivatives of an objective function with respect to the design variables and then using the calculated derivatives, or the "gradients," to determine the search path to find the next estimate of the optimal parameters. When the derivatives become zero, a local minimum has been found. Gradient-based approaches are usually computationally efficient in finding optimum solutions for continuous problems, but do not work well for discrete design problems where some parameters take values from a discrete set instead of continuous functions. The optimization problem studied in this research is generally of the mixed type where some design variables such as appliqué positions are continuous, but others may be discrete such as the number of appliqués. A non-gradient-based algorithm, namely the particle swarm optimization

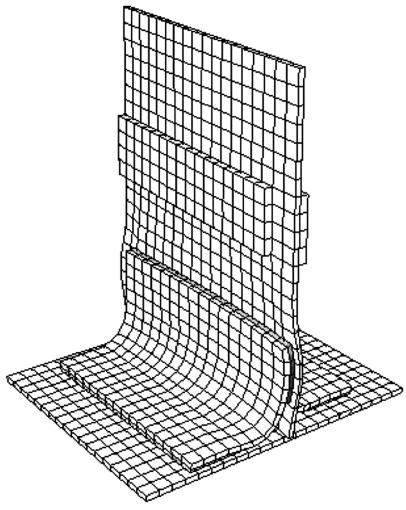

Fig. 3 Eliminating distortion due to clip misalignment by adding two appliqués.

(VisualDOC [10], Kennedy and Eberhart [12]) algorithm, was available when the number of appliqués was a design variable. This algorithm can handle either continuous or discrete design variables or a mixed problem.

In the context of the present problem, design variables could include shape, position, size, physical properties, the number of appliqués, etc. Increasing the number of design variables significantly increases the modeling complexity and computational cost. The analyst must use discretion in selecting variables. In the following sections, shape optimization and position optimization of the appliqués for the joint structure are discussed using a few modeling examples. It is shown that simple rectangular appliqués with only positions as design variables produced excellent results for the T-joint structure.

1. *Optimization With Respect to Appliqué Shape*

Throughout this study, the appliqués were assumed to be thin. Thick appliqués were found to have a complex three-dimensional response that was difficult and computationally expensive to account for. Restricting the methodology to thin appliqués is not considered a serious limitation.

Two rectangular appliqués were attached on each of the opposite faces of the T-joint vertical plate. In an attempt to optimize the appliqués' shape, perturbations were continually made to the corner points. The coordinates of all relevant nodes were changed so that the component's geometrical shape was correspondingly modified. For every new perturbed shape, ABAQUS performs an analysis of the deformation and feeds back the results to the optimization routine. This process continues until a minimization of the objective function for the structure has been achieved within the limitations of a fixed range of design variables. Figure 4 shows two initial rectangular appliqués added onto one surface of the vertical web.

Isoparametric mapping was used to compute the coordinate changes of all inner nodes due to the effect from perturbations on the corner node locations of the appliqués. The parametric coordinates of the nodes were taken as the same as those used to calculate the shape functions in common finite element analysis. The perturbations to all node coordinates were calculated following Leiva and Watson [13] and Candan et al. [14]. Linear modifications can be performed with the perturbations occurring only on the corner points. This technique transfers the initial rectangular shape into a new quadrilateral if the initial rectangular shape is treated as one domain or into a polygon if two domains are used. By resorting to higher-order mapping with midside node points also perturbed along with the corner points, the initial rectangular shape can be modified into a curved geometrical shape.

As an example, consider the thermal distortion of the T-joint structure assumed subject to a temperature change of 500°C. One possible measure of thermal distortion is the difference between the displacements of the two top corner nodes of the vertical plate. Note that a perfectly fabricated joint structure would be symmetric and this measure of distortion would be zero. For a defect, it is assumed that the two clips have a gross misalignment of 6 mm. The laminate and materials were assumed the same as described previously. Without the addition of antidistortion appliqués, the two out-of-plane displacements were computed as −0.03051 and 0.02325 mm. Defining the square of their difference as the objective function to be minimized the initial value was 0.002890.

With two appliqués added onto the two opposite surfaces of the vertical plate, as shown in Fig. 4a, optimization was performed with respect to both the position and shape of these appliqués. After optimization, the displacements were reduced to −0.00881 and 0.01452 mm. This reduced the objective function to 0.000544, which corresponds to an 81% reduction. The objective function history during the computations is shown in Fig. 5. As seen in Fig. 5, it is notable that most of the improvement came with initial placement of the appliqués (iteration 0). The optimized appliqués are illustrated in Fig. 4b. The improvement was substantial but the modeling effort required for the shape optimization was significant, and it was found later that using simple shapes with only position optimization was just as effective.

2. *Optimization with Respect to Appliqué Position*

For industrial applications, there would be some limitations on the appliqués. For example, the total area of the appliqués, the mass of the appliqués, and the relative positions of appliqués on the major components will all generally have limits. If the initial manufacture of the structure is conducted using basic methods for keeping the distortions small, then it is expected that the size and number of appliqués required to offset those distortions will be small. In the currently studied joint structure, it makes sense that the size of the attached appliqués should be much smaller than that of the major components. Small appliqués have more flexibility in their possible positions.

In this modeling exercise, a different composite material was selected that has almost null in-plane CTE, as studied by Ishikawa et al. [6]. The plates and clips are 20-ply laminates defined as $[+46.4/0/-46.4/0/+46.4/0/-46.4/0/+46.4/-46.4]_s$ where the 0 deg fibers all lie in the x-z plane of the coordinate system shown in Fig. 1. For example, for the vertical plate, the 0 deg fibers are parallel to the z axis. The plies were 60% fiber by volume. The mechanical and thermal ply properties were as follows: $E_{11} = 135$ GPa, $E_{22} = 11.0$ GPa, $v_{12} = 0.30$, $v_{23} = 0.59$, $G_{12} = 5.5$ GPa, $G_{23} = 3.17$ GPa, $\alpha_{11} = -0.26$ ppm, and $\alpha_{22} = 3.2$ ppm.

Figure 6 shows the magnified distortion state of the joint due to some misalignment of the two clips with the structure assumed to sustain a temperature change of 500°C. Two rectangular appliqués as initially randomly located on each side of the plate are included in Fig. 7. The optimization goal was to minimize the summation of the absolute displacement values of all the 19 topmost nodes (see Fig. 6) of the vertical plate. The optimization procedure was implemented with the positions of the four small appliqués as design variables. The initial and final displacement results obtained from the optimization procedure are listed in Table 1. It can be observed that the displacements of most nodes have been significantly decreased and their summation has been reduced by nearly an order of magnitude. Figure 8 illustrates the deformations of the joint after the four small rectangular appliqués on the two sides of the vertical plate have arrived at their optimal positions. Note that in Figs. 6–8, the

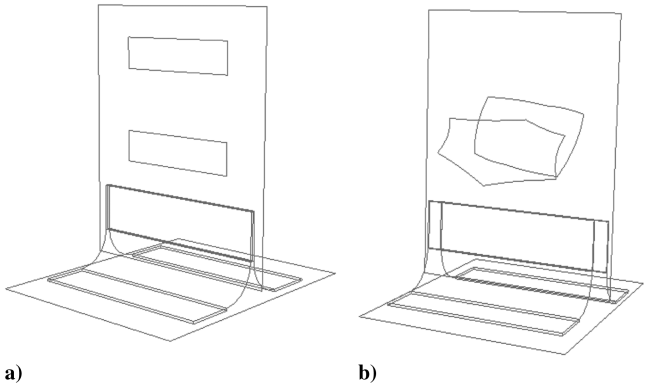

a) b)

Fig. 4 Two thin appliqués attached on the two surfaces of the plate: a) initial positions and shape, and b) final optimized positions and shapes.

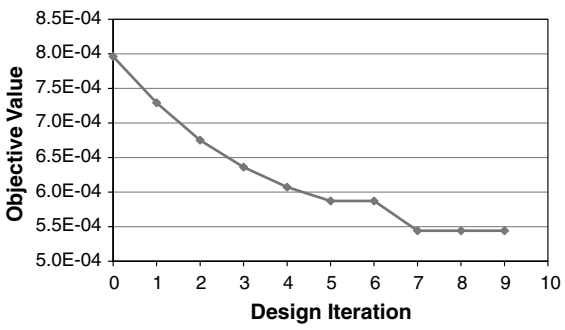

Fig. 5 Minimization of the objective $(U_{(1)} - U_{(2)})^2$.

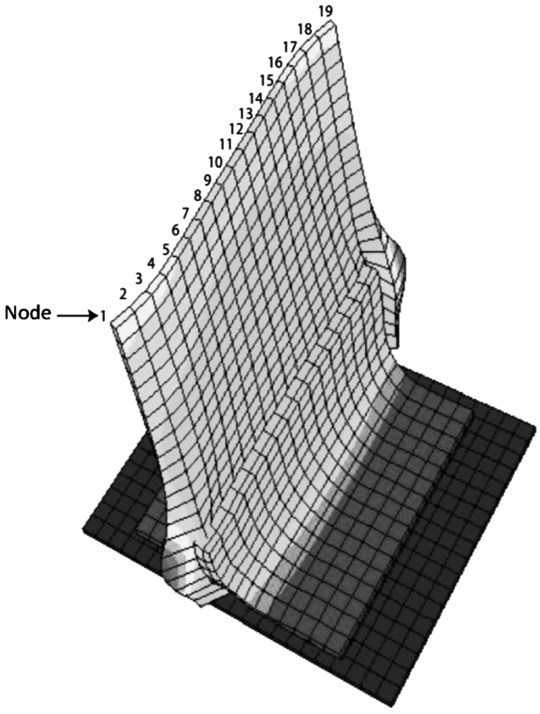

Fig. 6 Distorted joint due to clip misalignment.

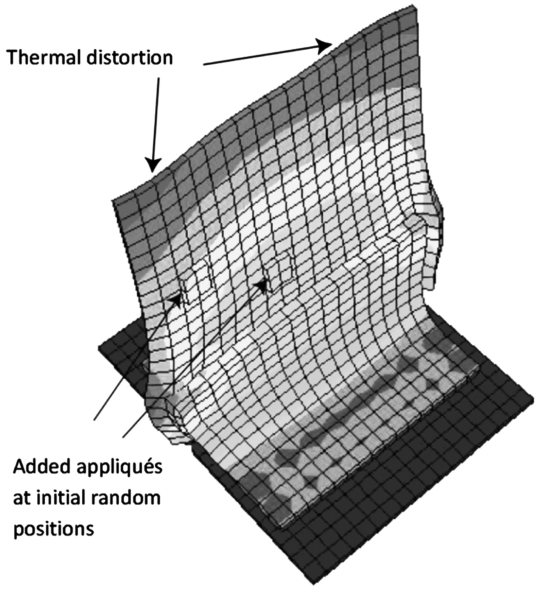

Fig. 7 Joint's initial state with appliqués added but before optimization.

deformations have been scaled by the same amount in each figure so that the differences can be visually compared.

F. Virtual Hardware Validation

A specific T-joint geometry was developed for experimental demonstration of the antidistortion appliqué methodology. To obtain measurable distortions, the T-joint was modified to include a metal foil covering a portion of one side of the vertical web. Photogrammetry was used to measure deflections due to temperature change. The photogrammetry system had an accuracy limit of about 0.028 mm. A finite element model of the joint indicated the metal foil would cause thermal distortion deflections about 1 order of magnitude larger so it was expected that they would be measurable within reasonable error. Several views of the finite element model with dimensions of the T-joint are shown in Fig. 9. Continuum shell elements [15] containing layers of integration points for each of the plies were used throughout the model. Shown in these figures are nominal dimensions of the actual assembly, including the titanium foil used to induce the out-of-plane distortions of the vertical plate. All the composite parts (baseplate, vertical web, and curved clips) were made up of a 48-ply laminate with a $([-45/0/45/90]_s)_6$ laminate sequence. The thermoelastic properties used in the analyses for the adhesive, the laminae, and the titanium foil are listed in Table 2.

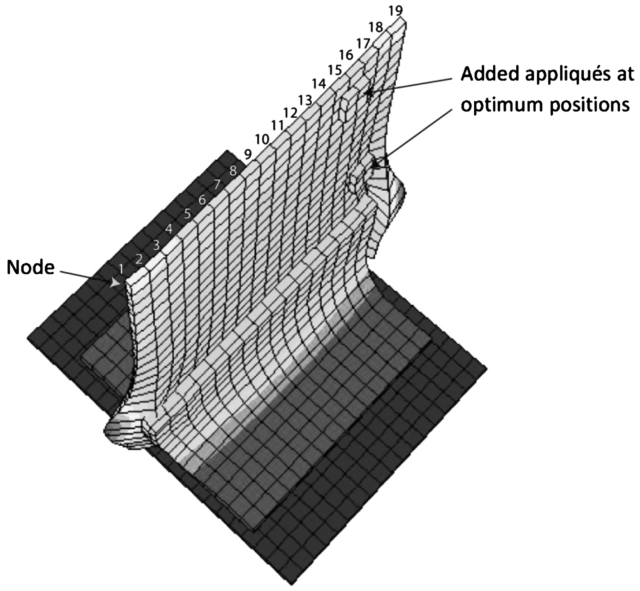

Fig. 8 Optimized structure after adding four small appliqués.

As a result of the previously described analyses, it was concluded that the most practical approach for implementing the antidistortion appliqué methodology was to use simple rectangular appliqués and limit the design variables to coordinate locations of the appliqués. Hence, this basic strategy was applied for the hardware demonstration. Of course, depending on the application, different materials might be used for the appliqués. For example, coupons of unidirectional composite would introduce anisotropy of the appliqué thermomechanical response and possibly be more effective in certain situations. Then, the appliqué orientation could also be an effective design variable in the optimization.

Before any testing, a purely analytical optimization was performed that mimicked the process eventually used on the actual part. The photogrammetry was capable of tracking a finite number of predefined target points. Nine target points were established on the foil side of the vertical web, as illustrated in Fig. 10. Deflections at these target points then serve as a basis for defining an objective function for the analysis. Physically, it was decided that the objective would be to keep the vertical plate flat with no regard for rigid body

Table 1 Out-of-plane nodal displacements for nodes at the top edge of the vertical plate (unit: 10^{-2} mm)

Node	*1*	*2*	*3*	*4*	*5*	*6*	*7*	*8*	*9*	*10*
No appliqués	−2.9	1.8	4.9	5.8	5.3	4.3	3.1	2.0	0.96	−0.01
With appliqués	−0.39	0.8	1.1	0.67	0.27	0.10	0.06	0.08	0.13	0.21
Node	*11*	*12*	*13*	*14*	*15*	*16*	*17*	*18*	*19*	*Sum*
No appliqués	−0.98	−2.0	−3.1	−4.3	−5.3	−5.8	−4.9	−1.9	2.9	**62.3**
With appliqués	0.30	0.39	0.38	0.08	0.18	0.18	−0.94	−1.6	−1.3	**9.12**

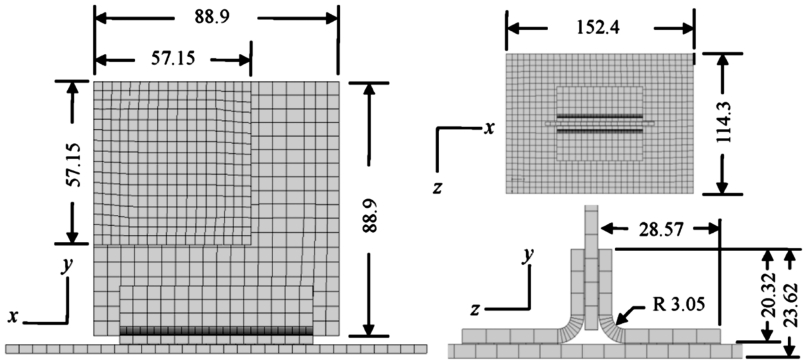

Fig. 9 Three views of the T-joint finite element model at three different scales showing the various plate and attached metallic foil dimensions in millimeters.

motion. Mathematically, this meant using three of the target points to define a plane and then minimizing the relative out-of-plane displacements of the remaining target points.

1. Numerical Implementation

In what follows, the objective function was defined in terms of the displacements at the nine target points used by the photogrammetry. Three of those points define a plane in the deformed coordinates. The points chosen to define a plane were b, d, and c, as labeled in Fig. 10. Using the coordinates of points b, d, and c, two position vectors in the plane were defined by Eqs. (1) and (2):

$$\mathbf{V}_1 = (x_b - x_d)\mathbf{i} + (y_b - y_d)\mathbf{j} + (z_b - z_d)\mathbf{k} \tag{1}$$

$$\mathbf{V}_2 = (x_c - x_d)\mathbf{i} + (y_c - y_d)\mathbf{j} + (z_c - z_d)\mathbf{k} \tag{2}$$

The vectors **i**, **j**, and **k** are unit vectors parallel to the x, y, and z coordinate axes. The unit normal that defines this plane was obtained from the normalized cross product of the vectors $\mathbf{V}_1$ and $\mathbf{V}_2$, and is given by Eq. (3):

$$\mathbf{u}_n = \frac{\mathbf{V}_1 \times \mathbf{V}_2}{|\mathbf{V}_1 \times \mathbf{V}_2|} \tag{3}$$

The position vectors from point d to each of the remaining points a, g, h, f, and e in the model are given by Eqs. (4–8). Note that the target point "i" was not considered in the objective function simply because it was thought, in error at the time, that this point could not be included in the experiments that were to follow:

$$\mathbf{V}_3 = (x_a - x_d)\mathbf{i} + (y_a - y_d)\mathbf{j} + (z_a - z_d)\mathbf{k} \tag{4}$$

$$\mathbf{V}_4 = (x_g - x_d)\mathbf{i} + (y_g - y_d)\mathbf{j} + (z_g - z_d)\mathbf{k} \tag{5}$$

$$\mathbf{V}_5 = (x_h - x_d)\mathbf{i} + (y_h - y_d)\mathbf{j} + (z_h - z_d)\mathbf{k} \tag{6}$$

$$\mathbf{V}_6 = (x_f - x_d)\mathbf{i} + (y_f - y_d)\mathbf{j} + (z_f - z_d)\mathbf{k} \tag{7}$$

Table 2 Thermoelastic material properties used in the finite element models

Property	Lamina	Adhesive	Al	Ti
E_{11}, GPa	207	2.07	72.4	116
E_{22}, E_{33}, GPa	10.3	2.07	72.4	116
υ_{12}, υ_{13}	0.3	0.41	0.33	0.36
G_{12}, G_{13}, GPa	2.76	0.734	27.2	42.6
υ_{23}	0.6	0.41	0.33	0.36
α_{11}, $\mu°C^{-1}$	−0.36	75.6	23.4	8.5
α_{22}, α_{33}, $\mu°C^{-1}$	27	75.6	23.4	8.5

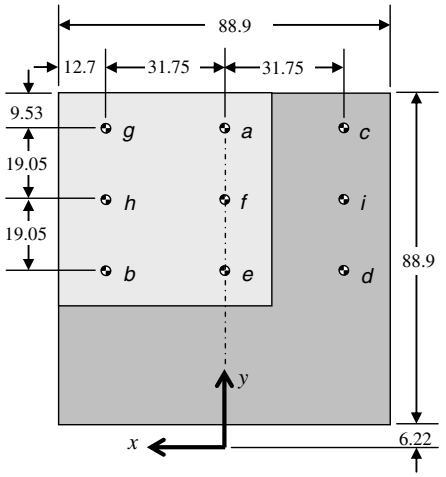

Fig. 10 Vertical plate showing the target point locations in millimeters.

$$\mathbf{V}_7 = (x_e - x_d)\mathbf{i} + (y_e - y_d)\mathbf{j} + (z_e - z_d)\mathbf{k} \tag{8}$$

The out-of-plane deflections of points a, g, h, f, and e were then obtained from the scalar product of the preceding position vectors and the unit normal vector. The objective function to be minimized was defined as the sum of the squares of the scalar products between the plane normal $\mathbf{u}_n$ and the vectors $\mathbf{V}_3$–$\mathbf{V}_7$. This results in the objective function defined by Eq. (9):

$$\text{Obj} = (\mathbf{V}_3 \cdot \mathbf{u}_n)^2 + (\mathbf{V}_4 \cdot \mathbf{u}_n)^2 + (\mathbf{V}_5 \cdot \mathbf{u}_n)^2 + (\mathbf{V}_6 \cdot \mathbf{u}_n)^2 + (\mathbf{V}_7 \cdot \mathbf{u}_n)^2 \tag{9}$$

The deformed coordinates were used to calculate the position vectors as just defined, which were used to compute the updated scalar value of the objective function. In an actual application of the method, the displacements would come from experiments that simulate the structure's application environment. These actual displacements would be added to the predicted displacement from the FEA model so that the minimization process would yield predicted displacements that cancel with the measured ones, yielding a net minimized distortion. Here, in a trial analysis, we used a virtual experiment and the appliqués are introduced to directly cancel with the simulated displacements. The aluminum foil was considered a gross defect that would warp the vertical web from its otherwise perfectly planar configuration. This "virtual" implementation of the antidistortion appliqué approach was performed in preparation for the actual physical testing and analysis of the T-joint.

2. Optimization with Three Appliqués

Three aluminum appliqués each of size 12.7 × 12.7 × 1.016 mm were modeled as attached to the vertical web on the side opposite to

Table 3 Displacement variables and deformed *x-y-z* coordinates input to the objective function where ω represents any target point *a–i*

FEA displacement due to titanium foil	Experimental displacement due to titanium foil	FEA displaced coordinate due to titanium foil and aluminum appliqués	Objective function input coordinate, Eqs. (1), (2), and (4–8)
$Ux\omega$	$\hat{U}x\omega$	$\hat{x}_\omega$	$x_\omega = \hat{x}_\omega - Ux\omega + \hat{U}x\omega$
$Uy\omega$	$\hat{U}y\omega$	$\hat{y}_\omega$	$y_\omega = \hat{y}_\omega - Uy\omega + \hat{U}y\omega$
$Uz\omega$	$\hat{U}z\omega$	$\hat{z}_\omega$	$z_\omega = \hat{z}_\omega - Uz\omega + \hat{U}z\omega$

the aluminum foil, as depicted in Fig. 11. Each of the appliqués was simulated as attached to the vertical web with a 0.254-mm-thick adhesive layer included. The objective function was minimized by altering the position of these three appliqués. The appliqués' positions were altered and the analysis was repeated as driven by the gradient-based optimization routine in VisualDOC. Figure 12 shows the numerical value of the objective function as the position of the appliqués was modified by the optimization routine. Ultimately, the objective function was reduced by approximately 90% by finding the optimal positions of the three appliqués. Relative to the center of the baseplate, the optimized (x, y) coordinate positions of the centers of the three appliqués were (−0.08, 73.45), (21.81, 61.08), and (−24.54, 75.68). It is notable that, for several random starting positions, the same minimum was found, suggesting that there were not multiple minima.

3. Optimization with Four Appliqués

For actual fabrication, titanium foil was selected instead of the aluminum modeled as described in the preceding paragraph. The properties of the titanium are shown in Table 2. Another "analysis only" optimization was conducted with titanium in the model and with four appliqués used instead of three. The thickness of the appliqués was reduced to 0.635 mm. The positions of the four appliqués were optimized to reduce the objective function defined earlier. Relative to the center of the baseplate, the optimized (x, y) coordinate positions of the centers of the four appliqués were (−2.91, 60.07), (18.53, 54.20), (−14.80, 50.32), and (−11.81, 29.97). Figure 12 shows the history of the magnitude of the objective function. The optimization reduced the objective function by 87.5%.

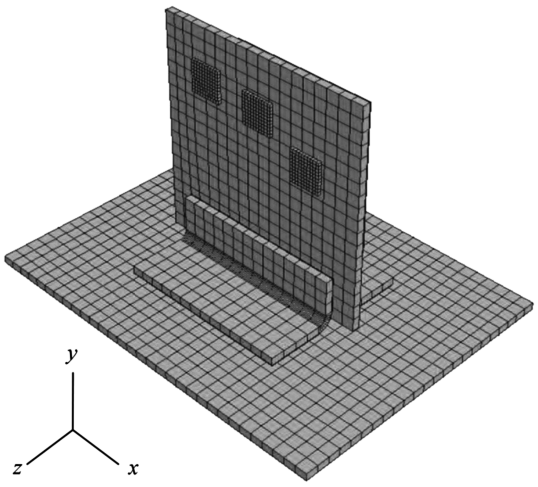

Fig. 11 FE model with optimized three-appliqué system.

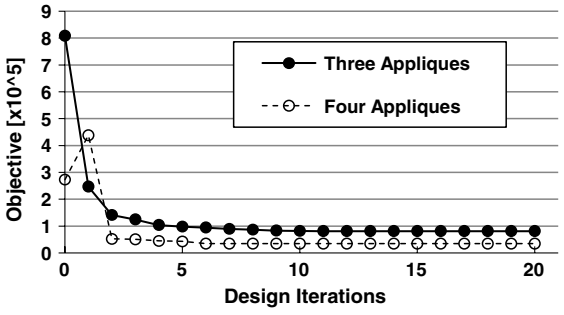

Fig. 12 Objective function as a function of design iterations.

G. Validation with Experiments

In the experiments, the laminate properties were different than those described previously and were held proprietary by an industry partner. The actual composite laminate was similar to a quasi-isotropic graphite-epoxy system modeled in the previous section. The target points used in this new objective are shown in Fig. 10. The objective function was in essence the same as defined by Eqs. (1–9). However, the input coordinates for Eqs. (1), (2), and (4–8) were adjusted so that the appliqué-driven displacements would, in their optimized locations, cancel with those measured in the laboratory, thus minimizing the out-of-plane distortion of the vertical plate. In contrast to the previous modeling-only studies, the simulated distortion due to the metal foil is not to be canceled by the appliqués. Hence, they were removed from the total deflection of the target points so that the only out-of-plane displacements were those measured experimentally and added in to the objective function. Then, the system of appliqués was optimized to produce displacements that cancel with the experimentally measured ones. The new objective function is the same as Eq. (9) but with input coordinates as defined in Table 3. Note that, in an actual application, the source of the distortion, in this case the metal foil, would not be in the model, and so there would be no need to subtract those displacements from the target point coordinates.

1. Experimental Results

Alliant Techsystems (ATK) Corporation conducted the photogrammetry experiments. The T-joint structure prepared for photogrammetry is shown in Fig. 13. The titanium foil can be seen on the vertical plate along with the nine target points where the displacements were measured. The target points are retroreflective tape and were 3 mm in diameter. The various target point patterns on the baseplate were necessary for the photogrammetry software to solve for the camera position. The T-joint was subjected to a

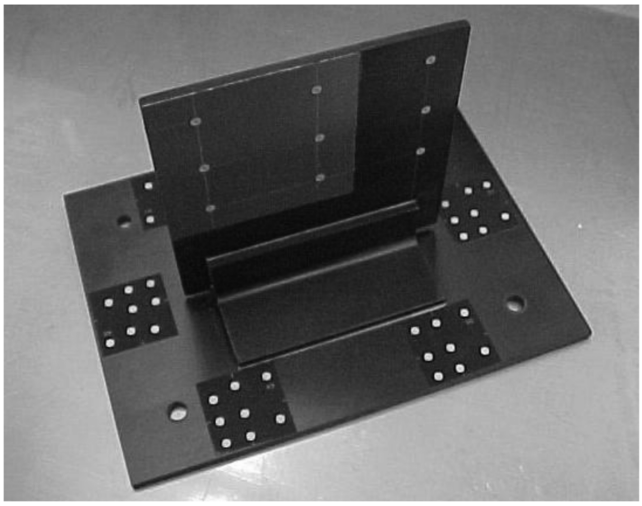

Fig. 13 Composite T-joint showing the titanium foil and nine target points on the vertical plate.

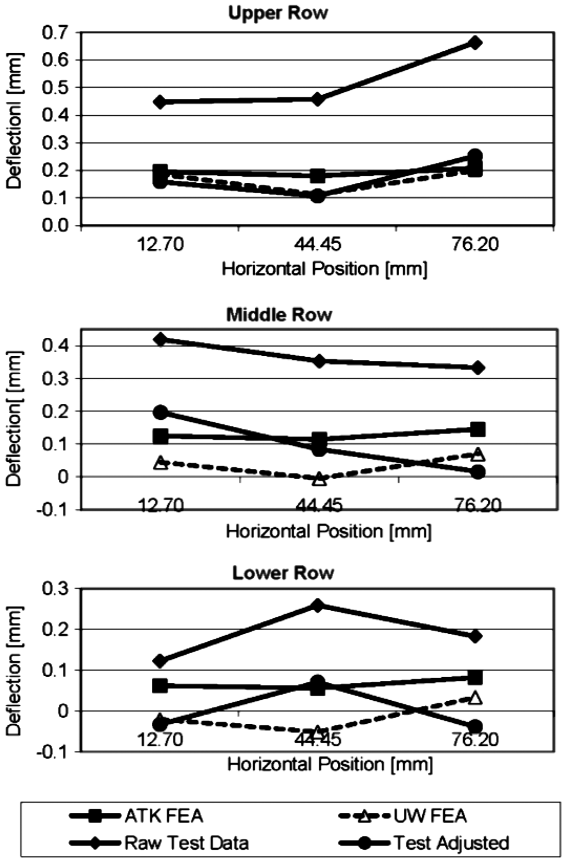

Fig. 14 Comparison of experimentally measured deflections and FEA predictions for the nine target points.

temperature change from 80 to −150 °C. The measured out-of-plane displacement data are summarized in Fig. 14. Only the displacements perpendicular to the web were of practical interest because they will dominate the characterization of the nonplanar distortion of the vertical plate. In Fig. 14, the raw displacements for each row of three points are shown which include displacement due to rigid body motion of the T-joint structure. Subsequently, the rigid body part of the total displacements was removed, and the resulting net displacements are include in Fig. 14 and are in reasonable agreement with independent finite element calculations performed at ATK and at the University of Wyoming (UW).

The top row of points, where the deflections were the largest, are in particularly good agreement with the results from the FE analyses. The bottom row has what could be described as an anomaly. The experimental data suggest that the web has a curvature opposite that of the other two rows and opposite that of the FEA predictions. The source of the anomaly is unknown. However, it is known that the statistical uncertainty of the experimental measurement was ±0.028 mm (±1 standard deviation) at −150°C compared with the small deflections occurring along the bottom row of target points (on the order of 0.050 mm). For this reason, point *e* was not included in the analysis. With that observation and the relatively good agreement with the other two target rows, the experiment was judged to have a level of success adequate for the purposes of the demonstration.

2. *Appliqué Position Optimization*

Two aluminum appliqués, 12.7 mm square and of 0.635 mm thickness were modeled as attached to the vertical web using an adhesive of 0.254 mm thickness. Larger numbers of appliqués were found to be ineffective in further reducing the objective function. To be effective, it was known that the appliqués would have to be on the side of the vertical plate opposite to the titanium foil. This is a departure from a real application where the sources of the distortion would generally be unknown and such beneficial judgment could not

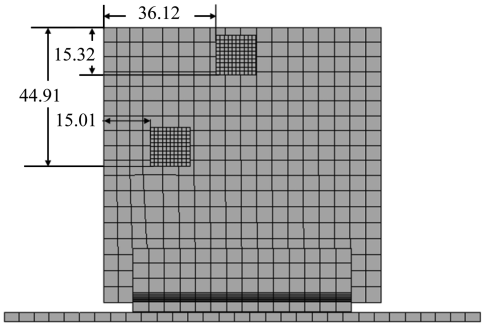

Fig. 15 FE mesh and optimized positions of two appliqués shown in millimeters.

be exploited. The optimization procedure was performed using VisualDOC combined with the ABAQUS FE model of the joint to minimize the objective function that relates to nonplanar distortion of the plate. The optimized positions of the appliqués resulted in an approximately 61% decrease in the objective function according to the model predictions. The optimized positions of the appliqués are as shown in Fig. 15.

The 61% decrease was much less than the decrease predicted previously with analysis-only optimization. It is believed that this can be attributed to the limitations of the photogrammetry system. The numerical optimization procedure attempts to eliminate the measured deflections. If components of those deflections are not real (experimental error), then they will generally be counter to the physics of the problem. Because the models presumably do a good job of simulating the physics, they will have extreme difficulty offsetting nonphysical deformations with the appliqués.

With the optimized positions of the two appliqués from the analysis, the experiment was repeated by subjecting the T-joint with appliqués added to a temperature change from 80 to −150 °C. The displacements at the target points were then used in Eq. (9), and it was found that the experimentally measured objective function was reduced by 78%.

III. Conclusions

An approach for improving static dimensional stability of composite structures was described. It was proposed that the as-built structure can be modified to remove dimensional instabilities stemming from inevitable manufacturing defects. The approach relies on a finite element representation of the idealized thermomechanical properties of the structure. The model can be idealized because it is unnecessary to simulate the sources of thermal distortion. In fact, the sources can be unknown. The model is then used to design modifications through material additions, referred to as antidistortion appliqués, which cause distortions opposite to those measured for the actual structure in the laboratory. To automate the process, optimization software was used in conjunction with the finite element software so that optimal configurations could be determined without trial-and-error efforts by an analyst.

It has been shown through several modeling examples that the adverse thermal distortions due to unwanted fabrication defects can be reduced through the addition of designed systems of small appliqués. Optimization through numerical modeling was shown to provide a systematic approach to reducing the unwanted thermal distortion and thus to improve the dimensional stability of space structures. For the examples given, simple rectangular appliqué systems were shown to have the potential to reduce distortions by approximately 90%. A subsequent hardware demonstration, though achieving an experimentally measured 78% reduction in the objective function, was less convincing due to the relative errors in displacements as predicted by two independent FEA solutions and as measured using photogrammetry in the laboratory. Still, this concept of antidistortion appliqués appears to have the potential of significantly improving space structures' dimensional stability.

This approach requires only the ability to model the structure's idealized thermomechanical properties, knowledge of the environmental stimulus (e.g., temperature change) that drives the instability, and a laboratory measurement of the instability to be eliminated. However, only measurable instabilities can be eliminated through this approach. This is, in fact, a major consideration of the approach because existing, more costly displacement measurement technology, beyond that which was used in this study, is needed for the precision of even moderately demanding applications.

Acknowledgment

The authors would like to thank the U.S. Air Force Office of Scientific Research, Grant FA 9550-04-1-0445, for support of this work.

References

[1] Prunty, J., "Dimensionally Stable Graphite Composites for Spacecraft Structures," *SAMPE Quarterly*, Vol. 9, No. 2, 1978, pp. 41–51.

[2] Maji, A., Kozola, B., and Griffin, S., "Design of Composite Surrogate Mirror Support Structure," *Journal of Aerospace Engineering*, Vol. 14, No. 3, 2001, pp. 112–118. doi:10.1061/(ASCE)0893-1321(2001)14:3(112)

[3] Dodson, K. J., and Rule, J. E., "Thermal Stability Considerations for Space Flight Optical Benches," *Proceedings of the 34th International SAMPE Symposium and Exhibition*, SAMPE International, Covina, CA, 1989, pp. 1578–1589.

[4] Shin, K.-B., Kim, C.-G., Hong, C.-S., and Lee, H.-H., "Thermal Distortion Analysis of Orbiting Solar Array Including Degradation Effects of Composite Materials," *Composites, Part B: Engineering*, Vol. 32, No. 4, 2001, pp. 271–285. doi:10.1016/S1359-8368(01)00020-8

[5] Grimaldi, F., Tempesta, G., Pastorelli, F., and Pesciarelli, S., "Development of Dimensionally Stable Lightweight Composite Satellite Antenna Structures," *Proceedings of the 34th International SAMPE Symposium and Exhibition*, SAMPE International, Covina, CA, 1989, pp. 1590–1602.

[6] Ishikawa, T., Fukunaga, H., and Ono, K.-I., "Graphite-Epoxy Laminates with Almost Null Coefficient of Thermal Expansion Under a Wide Range of Temperature," *Journal of Materials Science*, Vol. 24, No. 6, 1989, pp. 2011–2017. doi:10.1007/BF02385415

[7] Bansemir, H., and Haider, O., "Fibre Composite Structures for Space Applications: Recent and Future Developments," *Cryogenics*, Vol. 38, No. 1, 1998, pp. 51–59. doi:10.1016/S0011-2275(97)00110-0

[8] Yoon, K. J., and Kim, J.-S., "Effect of Thermal Deformation and Chemical Shrinkage on the Process Induced Distortion of Carbon/Epoxy Curved Laminates," *Journal of Composite Materials*, Vol. 35, No. 3, 2001, pp. 253–263. doi:10.1177/002199801772662244

[9] Farmer, J. T., Wahls, D. M., and Wright, R. L., "Thermal Distortion Analysis of an Antenna-Support Truss in Geosynchronous Orbit," *Journal of Spacecraft and Rockets*, Vol. 29, No. 3, 1992, pp. 386–393. doi:10.2514/3.26363

[10] VisualDOC Manual, Ver. 4, Vanderplaats Research & Development, Inc., Colorado Springs, CO, 2004.

[11] Matthews, F. L., Davies, G. A. O., Hitchings, D., and Soutis, C., "Finite Element Modeling of Composite Materials and Structures," Woodhead Publishing, Cambridge, England, U.K., 2000.

[12] Kennedy, J., and Eberhart, R. C., "Particle Swarm Optimization," *Proceedings of the IEEE International Conference on Neural Networks*, Vol. 4, Inst. of Electrical and Electronics Engineers, Piscataway, NJ, 1995, pp. 1942–1948.

[13] Leiva, J. P., and Watson, B. C., "Automatic Generation on Basic Vectors for Shape Optimization in the Genesis Program," AIAA Paper 98-4852, 1998.

[14] Candan, S., Garcelon, J., and Balabanov, V., and Venter, G., "Shape Optimization Using ABAQUS and VisualDOC," AIAA Paper 2000-4769, 2000.

[15] ABAQUS Analysis Users Manual, Ver. 6.5, ABAQUS, Inc., Providence, RI, 2004.

F. Pai
Associate Editor